

Cost-Effective Design of Grid-tied Community Microgrid

Moslem Uddin, Huadong Mo, and Daoyi Dong

Abstract—This study aims to develop a cost-effective microgrid design that optimally balances the economic feasibility, reliability, efficiency, and environmental impact in a grid-tied community microgrid. A multi-objective optimization framework is employed, integrating HOMER Pro for system sizing with deep reinforcement learning (DRL). Sensitivity analyses are conducted to evaluate the system performance under varying load demand and renewable energy fluctuations, while an economic sensitivity assessment examines the impact of electricity prices and capital costs on the Levelized Cost of Energy (LCOE). The proposed microgrid configuration achieves high reliability, satisfying 100% of the load, even under adverse weather conditions. The proposed framework attains an efficiency of 91.99% while maintaining a carbon footprint of 302,747 kg/year, which is approximately 95% lower than that of the grid system. The economic analysis indicates a net present cost (NPC) of \$4.83M with a competitive LCOE of \$0.208/kWh. In addition, the operation cost is \$201,473 per year with a capital investment of \$1.42M, rendering it a financially viable alternative to conventional grid-dependent systems. This work can be valuable in identifying effective solutions for supplying reliable and cost-effective power to regional and remote areas.

Index Terms—Microgrid, Multi-Objective Optimization, Cost-Effective Design, Renewable Energy, Energy Storage.

I. INTRODUCTION

THE global energy landscape is undergoing a rapid transformation toward decentralized, sustainable power systems that can meet increasing demands while mitigating environmental impacts [1–3]. Grid-tied community microgrids (MGs) represent a promising solution that enhances reliability and facilitates the integration of renewable resources. They also offer potential economic benefits to local communities [4–6]. These systems maintain a connection to the main utility grid while providing the capability to operate independently, when necessary. This hybrid approach ensures a balance between resilience and operational efficiency by integrating the grid connectivity with autonomous functionality [7]. However, designing economically viable community MGs remains challenging due to complex technical requirements, regulatory considerations, and financial constraints [8–11]. Therefore, cost-effective MG design has attracted much attention in global academic communities.

Moslem Uddin is with School of Engineering Technology, The University of New South Wales, Canberra, ACT 2610, Australia (email: moslem.uddin.bd@gmail.com).

Huadong Mo is with School of Systems and Computing, The University of New South Wales, Canberra, ACT 2610, Australia (email: huadong.mo@unsw.edu.au).

Daoyi Dong is with Australian AI Institute, FEIT, University of Technology Sydney, Sydney, NSW 2007, Australia (email: Daoyi.Dong@uts.edu.au).

A. Related work

In recent years, many studies have focused on cost-effective MG design. In [12], a predominantly renewable-energy-based MG was proposed for a residential community in Beijing. The proposed MG demonstrated the capability to supply a minimum of 90% of the electricity demand utilizing 47–100% renewable sources, with a moderately sized battery system proving to be more cost-effective than a system without energy storage capabilities. Liu et al. [13] proposed a system parameter design approach for community MGs based on a bi-level optimization model that effectively enhances reliability and reduces operation costs without increasing customers' power consumption expenditures. In the proposed approach, the optimal system configuration and operational parameters are generated in an integrated manner. A co-optimization strategy was proposed for distributed energy resource planning to minimize the total annualized cost while maximizing fuel savings [14]. Lagrange multipliers were utilized to maximize fuel savings by satisfying Karush–Kuhn–Tucker conditions. By applying Fourier transform and particle swarm optimization, the optimal combination of distributed energy resources was determined to reduce the annualized cost. Mohamed et al. [15] proposed an efficient planning algorithm for MGs. The algorithm ensures reliable power flow with minimal costs by determining the optimal grid topology, equipment allocation, and sizing while optimizing nonlinear scheduling problems for installed equipment. The Harris Hawks Optimization (HHO) algorithm was employed for sizing optimization and the design of an autonomous AC MG [16]. The HHO algorithm demonstrated the cost-effectiveness of the design, yielding savings ranging from 1.18% to 18.23% of the total NPC. However, environmental impact and efficiency constraints have not been explored. Considering environmental impact, a probabilistic approach was proposed for optimal sizing and techno-economic assessment of PV-based MGs [17]. Considering the environmental impact and reliability, a probabilistic approach was proposed for the optimal sizing and techno-economic assessment of PV-based MGs [17]. However, the scalability of this approach for multi-energy MGs requires further investigation. In [18], a novel Vectorial MG Optimization (VMO) method was proposed that optimized MG designs for critical loads by balancing the power supply availability, NPC, and power efficiency, thereby achieving high reliability and economic viability. Zhu et al. [19] established a stochastic multi-objective sizing optimization (SMOS) model for MG planning, which comprehensively incorporates the battery degradation characteristics and the total carbon emissions. A self-adaptive

multi-objective genetic algorithm (SAMOGA) was developed to solve the SMOSO model. In [20], a planning approach was proposed for a gas-electric-based integrated multi-energy system with a MG to enhance the resilience of the power grid against serious failures. The method uses mixed-integer linear programming (MILP) to establish an operational process based on the required resilience level and determine the optimal asset locations in the MG. Er et al. [21] employed a two-stage stochastic programming approach with scenario-based modeling to address a multi-energy system. The proposed design aims to minimize costs and maximize the system reliability. A modified bio-inspired optimization algorithm was employed to design a hybrid energy MG [22]. The efficacy of the proposed design was evaluated through a sensitivity analysis. In [23], a cost-effective MG was designed by considering multiple factors, including cost, resilience, and environmental impact. An innovative methodology for incorporating social dynamics into the design of community MGs utilized MILP [24]. Despite providing valuable insights into cost-effectiveness, most studies have primarily focused on minimizing costs and emissions. Furthermore, the reliability of MG design has not yet been adequately explored. Additionally, there is a paucity of studies in the literature that have considered MG efficiency issues during the design process, which can lead to suboptimal performance of the MG system. This suggests that research on this issue is still in its nascent stages and there are numerous unresolved challenges that require attention. Therefore, this study proposes a comprehensive design framework for multi-energy community MGs that integrates all the aforementioned factors.

B. Motivation

The increasing demand for sustainable, cost-effective, and resilient energy systems has led to the widespread adoption of MGs as viable solutions for decentralized energy management. However, extant MG design methodologies frequently prioritize individual performance factors, such as economic feasibility, environmental sustainability, efficiency, and reliability, rather than synergistically integrating all the four aspects. This fragmented approach constrains the potential for MGs to operate optimally in dynamic and uncertain energy environments. Fig. 1 presents a comparative analysis of the design approaches.

C. Contribution

This study aims to develop a comprehensive cost-effective design framework for grid-tied community MGs, ensuring economic feasibility and environmental sustainability without compromising reliability and efficiency. The proposed design framework facilitates financially viable MG deployment for residential communities. In summary, the main contributions and originality of this study are as follows:

- An optimal design method is developed, resulting in Pareto fronts of trade-offs between multiple objectives.
- Mathematical modeling is rigorously explained to provide a comprehensive understanding of complex MG systems, taking into account practical operational constraints.

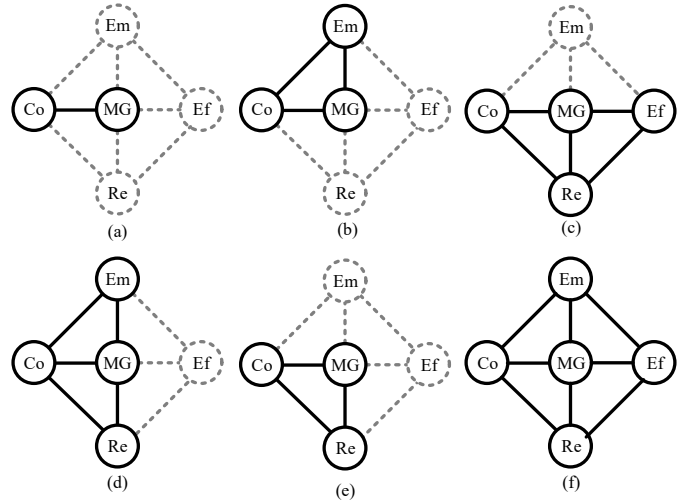


Fig. 1: Comparative Analysis of MG Design Approaches: (a) MG design prioritizing economic factors alone, (b) MG design integrating both economic and environmental considerations, (c) MG design that incorporates economic aspects alongside reliability and efficiency metrics, (d) MG design that merges economic considerations with environmental and reliability aspects, (e) MG design emphasizing economic and reliability factors, (f) Proposed MG design framework that synergistically combines economic, environmental, efficiency, and reliability factors for optimized performance. [Co →Cost, Em→Emission, Ef→Efficiency, and Re→Reliability].

- A thorough cost-benefit analysis is conducted, evaluating system performance in terms of NPC, LCOE, and reliability metrics.
- The proposed approach is validated utilizing real-world data and simulations, demonstrating its efficacy in reducing operational costs while ensuring energy security for community-scale applications.

II. PROBLEM FORMULATION

In this section, a multi-objective optimization framework is developed to optimally size the PV system, wind turbine (WTs), diesel generator (DG), grid converter, and battery of a community MG, considering a maximum grid capacity constraint. The optimization problem is initially defined, followed by a discussion of the objectives and variables. In the subsequent, the developed multi-objective optimization framework is employed to optimally size the MG components under various operational scenarios, while adhering to the maximum grid capacity limit.

A. Problem Statement

The increasing demand for reliable, efficient, and sustainable energy in residential communities necessitates innovative solutions to address the challenges of increasing energy costs, environmental impact, and the need for an uninterrupted power supply. Conventional energy systems predominantly rely on fossil fuels, resulting in high operational costs C_f and substantial carbon emissions CO_2 . Furthermore, these systems

are susceptible to reliability issues, particularly in remote or underserved areas. Hybrid MGs, which integrate multiple energy sources, such as photovoltaic (PV) solar, $P_{PV}(t)$, wind generation, $P_{wt}(t)$, backup DGs $P_{dg}(t)$, and battery storage $E_{bess}(t)$, offer a promising solution. However, designing such systems to achieve cost-effectiveness while optimizing reliability, efficiency, and emissions reduction presents a complex challenge.

B. Decision Variables

In the context of designing and optimizing hybrid MGs for residential communities, the decision variables are of paramount importance in defining the operational and planning aspects of the system. Decision variables are categorized into two distinct sets: binary decision variables \mathbf{Y} and continuous decision variables \mathbf{X} . Binary decision variables \mathbf{Y} indicate the selection of specific energy sources in the hybrid MG system. This can be mathematically represented as follows:

$$\mathbf{Y} = \{(i, y_i) \mid i \in \{\text{PV, WT, DG, BESS}\}\} \quad (1)$$

where $y_i \in \{0, 1\}$. Condition $y_i = 1$ indicates that the energy source i is incorporated into the system, whereas $y_i = 0$ signifies its exclusion.

The continuous decision variables \mathbf{X} define the operational levels of energy sources over time. This is represented by:

$$\mathbf{X} = \{(i, x_i) \mid i \in \{\text{PV, WT, DG, BESS}\}\} \quad (2)$$

where $x_i(t)$ denotes the output of energy source i at time t . These variables are further constrained within operational limits and are time-dependent.

C. Objective Functions

The proposed sizing tool is developed to provide the optimal PV, wind, diesel, BESS, and grid capacity under objective function (F_{obj}) described by Eq. (7). The coefficients are employed as normalization factors to ensure the same order of magnitude for all summation terms. The determination of the MG architecture and sizing of energy resources is contingent upon balancing four critical performance metrics: minimizing the NPC (C_{NPC}) and carbon emissions (ΔCO_2), while maximizing the power supply reliability (\mathcal{R}_{sys}) and the system efficiency (η_{sys}). Consequently, the MG design problem can be formulated as a multi-objective optimization model as follows:

$$F_1 = [\min C_{NPC}] \quad (3)$$

$$F_2 = [\max \mathcal{R}_{sys}] \quad (4)$$

$$F_3 = [\max \eta_{sys}] \quad (5)$$

$$F_4 = [\min \Delta CO_2] \quad (6)$$

$$F_{obj}(X, Y) = [F_1, F_2, F_3, F_4] \quad (7)$$

Algorithm 1 Optimized Grid Search for Feasible MG Designs

- 1: **Input:** Technical characteristics and economic data for MG components.
- 2: **Define search spaces:**
 - Grid capacity, $S_{grid} = \max(C_{dg})$
 - PV capacity, $S_{pv} = [\min_{pv}, \max_{pv}, \Delta_{pv}]$
 - WT capacity, $S_{wt} = [\min_{wt}, \max_{wt}, \Delta_{wt}]$
 - DG capacity, $S_{dg} = [\min_{dg}, \max_{dg}, \Delta_{dg}]$
 - Consumer demand, $S_{con} = [\min_{con}, \max_{con}, \Delta_{con}]$
 - BESS capacity, $S_{bess} = [\min_{bess}, \max_{bess}, \Delta_{bess}]$
- 3: **for** each configuration in the multidimensional search space **do**
- 4: Evaluate the technical and economic feasibility of the configuration
- 5: **if** configuration meets all constraints **then**
- 6: Record the configuration along with performance metrics
- 7: **end if**
- 8: **end for**
- 9: **Output:** List of all feasible configurations with their respective metrics

$$\begin{aligned} \text{subject to } & \sum_i x_i \cdot y_i \geq P_{load}, \\ & 0 \leq x_i \leq y_i \cdot P_{i,max}, \\ & \sum_i C_{cap,i} \cdot y_i + \sum_i C_{op,i} \cdot x_i + \sum_i C_{om,i} \cdot x_i \leq B, \\ & y_i \in \{0, 1\}. \end{aligned}$$

Since C_{NPC} , \mathcal{R} , η and ΔCO_2 are conflicting metrics, the outcome of optimization model will comprise non-dominated Pareto points, wherein an improvement in one metric necessitates a degradation in others. To facilitate the selection of an optimal MG design (S^*) within the Pareto set derived from 7, the normalized values of the multiple objectives can be aggregated into a single-objective scalar function as follows:

$$S^* = \min_{X,Y} [w_1 \bar{C}_{NPC} + w_2 \bar{\mathcal{R}}_{sys} + w_3 \bar{\eta}_{sys} + w_4 \Delta \bar{CO}_2].$$

where w_1 , w_2 , w_3 , and w_4 are the weighting coefficients utilized to assign a preference order to the performance metrics, considering the following:

$$w_1 + w_2 + w_3 + w_4 = 1, \quad w_i \in (0, 1) \quad (8)$$

III. PROPOSED METHODOLOGY

Multi-objective optimization of the community MG was addressed using a Pareto front approach enhanced by HOMER Pro simulations and DRL. The objectives are to minimize costs, reduce emissions, improve reliability, and enhance efficiency. HOMER generates diverse MG configurations, providing metrics for total cost, CO_2 emissions, reliability metrics, and system efficiency, whereas the DRL framework dynamically optimizes operational decisions to achieve Pareto-optimal solutions across the defined objectives. In HOMER Pro, a grid search algorithm (Algorithm 1) is utilized to identify all feasible designs based on the constraints defined for the analysis.

Algorithm 2 Optimal Configuration Using Derivative-Free Optimization

- 1: Initialize the optimal configuration and size for each component as the default configuration and size.
 - 2: Calculate the initial C_{NP} of the MG over the simulation period based on the default configuration and size.
 - 3: **for** $n = 1$ to maximum years of analysis **do**
 - 4: Calculate the C_{NP} of the MG over the simulation period based on the new configuration and size.
 - 5: If the new C_{NP} is greater than the current optimal C_{NP} , update the optimal configuration and size, and update the optimal C_{NP} .
 - 6: **end for**
 - 7: Set the component's capacity to the optimal capacity.
 - 8: Record optimal component sizes and metrics.
-

Subsequently, a proprietary derivative-free optimization algorithm Algorithm (2) determines the least-cost configuration with the highest reliability. This process is iteratively repeated in HOMER Pro for various sensitivity variables. Using RL, the optimization process dynamically explores and learns trade-offs between conflicting objectives, forming a Pareto front where no objective can be improved without compromising the others. The DRL framework adaptively adjusts decision policies to highlight trade-offs and achieves balanced solutions across multiple objectives. This approach is detailed in Algorithm 3. The Pareto front facilitates informed decision-making by enabling the selection of optimal configurations that balance strategic priorities in multi-objective MG optimization. It provides a robust framework to address complex trade-offs among cost, reliability, efficiency, and emissions. The trade-offs approach, enhanced by the integration of DRL, provides a dynamic and adaptive framework for designing sustainable and resilient MGs.

A. Design case study

The rural Australian community of Central Tilba in New South Wales, with 288 residents close to the Princes Highway, is considered as the case study for this research. This rural area still suffers from a lack of reliable and cost-effective electrical access despite being recognised as one of Australia's top cultural sites. The following sections detail the village's environmental and meteorological characteristics, community requirements, and suggested MG structures. Power demand analysis of end users and presenting a realistic electrical load model are crucial aspects of these investigations. This model assumes the large residential community's electrical load may not have changed substantially in recent years. The average daily power consumption is about 3139.3 kW/day, and the peak load is 235.2 kW. Fig. 2 illustrates the load profile of the case study rural community. The daily electrical loads also follow the oscillating distribution, with higher power demand during the daytime and less at night, with the peak load concentrating between 5:00 PM to 9:00 PM. Monthly solar radiation profile and ordinary wind velocity of Central Tilba, NSW (36°18.8'S, 150°04.6'E) are considered for this

Algorithm 3 Policy Gradient for Pareto Front Analysis

- 1: **Input:** Environment states, actions, rewards for cost, reliability, efficiency, emissions
 - 2: **Initialize:** Policy parameters θ , learning rate α
 - 3: **while** not converged **do**
 - 4: Generate episode data based on current policy π_θ
 - 5: Calculate cumulative rewards for each objective:
 - 6: $C_{NP}, \mathcal{R}_{sys}, \eta_{sys}, \Delta CO_2$
 - 7: Compute advantage estimates for each objective
 - 8: Perform policy gradient update:
 - 9: $\theta \leftarrow \theta + \alpha \nabla_\theta \log \pi_\theta(a|s) A(s, a)$
 - 10: **end while**
 - 11: **Generate multi-objective rewards:**
 - 12: **for** each action in the action space **do**
 - 13: Simulate environment response for action
 - 14: Record outcomes for all objectives
 - 15: **end for**
 - 16: **Identify Pareto-optimal solutions:**
 - 17: Construct the set of all feasible solutions
 - 18: Apply a Pareto optimality filter to identify non-dominated solutions
 - 19: **Output:** Set of Pareto optimal solutions with respect to the objectives
-

work. Solar and wind resource data are obtained from the NASA prediction of Worldwide energy resource database. The monthly average solar radiation and wind speed for this region are shown in Fig. 3.

B. MG Element Models

This subsection presents the system component models and the design considerations employed in the proposed approach to calculate the NPC, supply reliability, system efficiency, and carbon reduction of the MG for Central Tilba, NSW, Australia.

1) *PV Module:* Flat PV panels are selected for this study due to their are readily available on the local market. Detailed information about the PV module is given in Table I. The power output of a PV module is estimated considering the temperature influences on it. The following equation is used to calculate the output of the PV module [25]:

$$P_{pv} = Y_{pv} f_{pv} \left(\frac{\bar{G}_t}{\bar{G}_{t, std}} \right) [1 + \alpha_p (T_c - T_{c, std})]. \quad (9)$$

2) *WT Model:* Wind speeds at heights greater than 10 m are needed to produce efficient wind energy. However, the data was acquired with a 10 m standard anemometer. Therefore, hub height wind speeds at a potential location are derived using the well-known power law,

$$U_H = U_A \times \left(\frac{Z_H}{Z_A} \right)^\alpha \quad (10)$$

where U_H refers the wind speed at the hub height of the WT and U_A signify the wind speed at anemometer height, measured in meters per second (m/s). Similarly, Z_H and Z_A symbolize the hub height and the anemometer height of the WT respectively in m . The power law exponent is represented

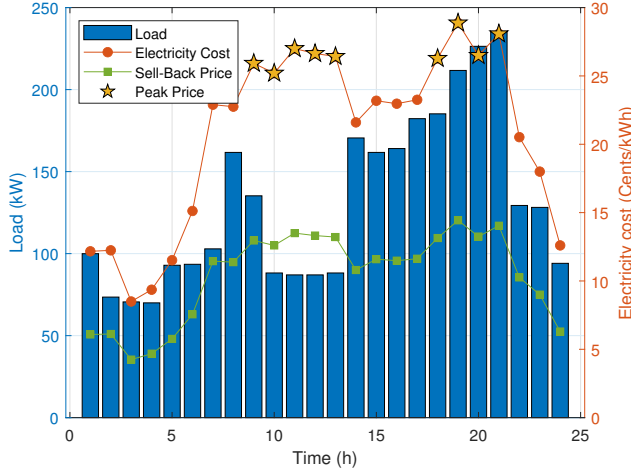


Fig. 2: Hourly Electrical demand and electricity price (\$), sellback price for the case study community.

by α . The exponent value of 0.14, or $(1/7)$, has been widely accepted as an accurate reflection of the prevalent conditions. U_H , ρ , and A_S , all influence the power production of WT. Therefore, the maximum P_{wt} can be expressed by the Eq. (11) [26]:

$$P_{wt} = \frac{1}{2} \rho A_S U_H^2. \quad (11)$$

where, A_S is swept area of rotor.

3) *DG Model*: In this investigation, a 60 kW Caterpillar DG generator is selected. The features of DG are listed in detail in Table I. To avoid damaging the generator's exhaust system, the minimum load ratio is set to 25%. The hourly fuel consumption of the DG can be mathematically described using a linear law [25]. This model is based on the power required by the load:

$$C_{DG}(t) = \alpha_{DG} \mathcal{P}_{DG, \text{rat}}(t) + \beta_{DG} \mathcal{P}_{DG, \text{out}}(t) \quad (12)$$

where α_{dg} indicates generator fuel curve intercept coefficient ($L/hr/kW_{\text{rated}}$) and β_{dg} refers to generator fuel curve slope ($L/hr/kW_{\text{output}}$). These two coefficients are provided by the manufacturer. While, $P_{dg}^{\text{rat}}(t)$ and $P_{dg}^{\text{out}}(t)$ are rated capacity and generated power output of DG in kW at time step t . Values of α_{dg} and β_{dg} are provided by the manufacturer.

4) *BESS Model*: In this study, the battery-charging process commences when power generation exceeds consumption. Conversely, when the renewable system is unable to meet energy demands, the storage system supplies the load. The battery state of charge (SOC) is used to establish the charge and discharge limits. Battery capacity is defined as the maximum extractable charge from a fully charged battery. Using Eq. 13, the maximum load power of the storage system can be determined [27].

$$P_b(t) = \frac{kQ_1(t)e^{-kt} + \bar{Q}(t)kc(1 - e^{-k\Delta t})}{1 - e^{-k\Delta t} + c(k\Delta t - 1 + e^{-k\Delta t})} \quad (13)$$

where $Q_1(t)$ represents the available energy at the start of the operational range that exceeds the minimum SOC. For Lithium-Ion batteries, the minimum SOC is 20%, whereas the

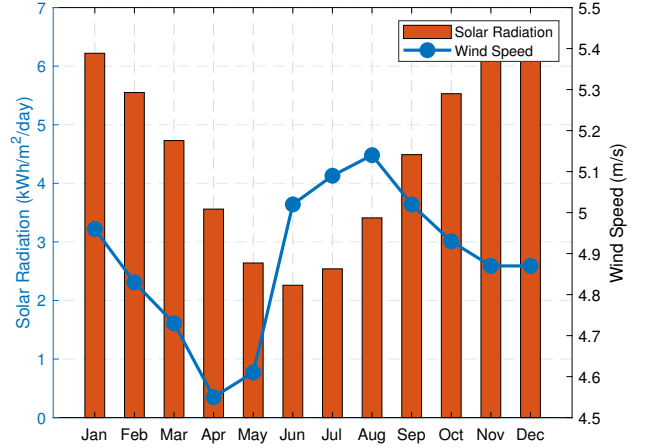


Fig. 3: Daily Average Solar Radiation and Wind Speed for the Case Study Community.

maximum SOC is 80%. $\bar{Q}(t)$ denotes the total energy at the initial time step, c corresponds to the storage-capacity ratio of each system, and k represents the constant energy-storage rate. Δt is the time interval under consideration. The maximum power output of a storage system can be determined using the following equation [27]:

$$P_b(t) = \frac{kQ_m(t)e^{-kt} + kQ_1(t)e^{-kt} + \bar{Q}(t)kc(1 - e^{-k\Delta t})}{1 - e^{-k\Delta t} + c(k\Delta t - 1 + e^{-k\Delta t})} \quad (14)$$

where $Q_m(t)$ is the total storage capacity. To ascertain the requisite number of batteries (N_b), it is essential to consider factors such as the operational lifespan of the hybrid system and longevity of each individual battery.

$$N_b = \left\lceil \frac{SH \cdot V_{ida}^{\text{pu}} \cdot a\tilde{n}o}{r_{\text{vida}}^b \cdot V_{ida}^b} \right\rceil \quad (15)$$

5) *Converter Model*: The converter model is crucial for the efficient operation of the MG, as it governs the conversion of power between DC and AC forms. The efficiency of this conversion process and the associated power losses are significant factors that impact the overall performance and reliability of the MG system. The output power $P_{\text{out}}(t)$ at any given time t is determined by the following equation:

$$P_{\text{out}}(t) = \eta_{\text{conv}}(t) \cdot P_{\text{in}}(t) - P_{\text{loss}}(t). \quad (16)$$

where $P_{\text{out}}(t)$ represents the power available for use after conversion, which is influenced by the efficiency $\eta_{\text{conv}}(t)$ of the converter at that specific time. The efficiency $\eta_{\text{conv}}(t)$ can vary due to several factors, including changes in load demand, environmental conditions, and the operational state of the converter. Additionally, $P_{\text{loss}}(t)$ accounts for the power losses that occur during the conversion process. These losses can arise from various sources such as resistance, heat dissipation, and other inefficiencies inherent in the converter's operation.

C. Performance Metrics and Evaluation Techniques

Diverse performance metrics and evaluation techniques are used to assess the effectiveness and efficiency of the MG system. The metrics under consideration include:

1) *MG Economic Performance*: Evaluating the economic performance of the MG is a crucial aspect of its overall feasibility and sustainability. The NPC is a widely used metric to assess the total cost of owning and operating a MG over its lifetime. The NPC is calculated using the following equation:

$$C_{NP} = \sum_{t=0}^T \frac{C_{tot}(t) - S(t)}{(1+r)^t}. \quad (17)$$

where $C_{tot}(t)$ denotes the total cost at time t . The salvage value $S(t)$ at time t is the residual value of the MG's components at the end of their useful life, recoverable through resale or recycling. The discount rate r accounts for the time value of money, reflecting a decrease in the present value of future costs and savings. The total project lifetime T is the duration over which the MG's economic performance is evaluated.

The total cost $C_{tot}(t)$ comprises multiple cost components, each representing a significant financial aspect of the MG operation.

- **Capital Cost** (C_{cap}): This represents the initial capital investment required for the establishment of the MG, encompassing equipment procurement, installation, and other associated capital expenditure.
- **Operation and maintenance cost** C_{OM} : It encompasses the ongoing operational expenditure essential for the efficient and reliable functioning of the MG, including routine maintenance procedures.
- **Fuel cost** $C_{fuel}(t)$: This accounts for the fuel expenditure required for generators and other fuel-dependent components within the MG system.
- **Replacement cost** $C_{rep}(t)$: This includes the costs associated with replacing or upgrading system components that have reached the end of their operational lifespan over the project duration.

By calculating the sum of the discounted total costs and subtracting the salvage values over the lifespan of the project, NPC provides a comprehensive measure of the long-term economic performance of the MG. This metric facilitates the comparison of various design alternatives and enables informed decision-making regarding the viability and cost-effectiveness of MG projects.

2) *MG Power Supply Reliability*: In this study, the reliability and resilience of MG systems are evaluated by employing the loss of power supply probability (LPSP) indicator as a quantitative metric. Eq. (18) is used to determine MG reliability as a function of LPSP.

$$\mathcal{R}_{sys} = e^{-\lambda \cdot LPSP} \quad (18)$$

where λ represents a scaling factor that modulates the rate of reliability decrease as the LPSP. The LPSP quantifies the proportion of the total energy demand that is not met by the MG over a specified period. It measures the probability of power shortages due to insufficient energy generation or storage. It is calculated as:

$$LPSP = \left(\frac{\int_0^T \max(0, P_{load}(t) - S(t)) dt}{\int_0^T P_{load} dt} \right) \times 100$$

TABLE I: Technical characteristics and economic data for MG components.

MG Components	Characteristics	Values	Unit
PV module	Nominal power, P_{pv}	1kW	kW
	Derating factor	80	%
	Capital cost	1300	\$/kW
	Replacement cost	1300	\$/kW
	O&M cost	10	\$/kW
WT	Lifetime	20	Year
	Nominal capacity, P_r	3	kW
	Cut-in wind speed, V_{ci}	4	m/s ²
	Cut-out wind speed, V_{co}	24	m/s ²
	Hub height, h	15	m
	Capital cost	2300	\$/kW
	O&M cost	207	\$/kW/year
DG	Lifetime	20	Year
	Nominal capacity, C_{deg}	60	kW
	Capital cost	400	\$/kW
	Replacement cost	400	\$/kW
Battery Storage	O&M cost	0.03	\$/h/kw
	Nominal capacity, C_{batt}	1	kWh
	Nominal voltage, V_{batt}	24	V
	Roundtrip efficiency, η_{RT}	90	%
	DoD	80	%
	Capital cost	700	\$/kW
	Replacement cost	700	\$/kW
	O&M cost	10	\$/year/kWh
Power converter	Lifetime	10	Year
	Nominal Capacity	1	kW
	Conversion efficiency, η_{inv}	95	%
	Capital cost	300	\$/kW
	Replacement cost	300	\$/kW
	O&M cost	0	\$/year
	Lifetime	15	Year

where P_{load} and $S(t)$ are the demand and supply of MG at time t respectively. T denotes the total time period.

3) *MG Efficiency* (η_{sys}): This metric is employed to assess the comprehensive energy efficiency of the MG system, encompassing factors such as energy loss, energy generation in relation to consumption, and overall system efficiency. η_{sys} is derived as follows:

$$\eta_{sys} = \left(\frac{\int_0^T P_{useful}(t) dt}{\int_0^T (P_{input}(t) - P_{loss}(t)) dt} \right) \times 100\% \quad (19)$$

where $P_{useful}(t)$ refers to the instantaneous useful power delivered to the load, $P_{input}(t)$ denotes the instantaneous total input power from all energy sources, and $P_{loss}(t)$ represents the power losses due to transmission, conversion inefficiencies, and storage losses.

4) *Environmental Impact*: The detailed equation for the reduction in carbon emissions ΔCO_2 due to the adoption of renewable energy sources (PV and wind) in the MG:

$$\Delta CO_2 = \left(\sum_{i \in \{PV, WT\}} (E_i \cdot \eta_i \cdot (1 - d_i) \cdot t \cdot EF_{grid}) \right) - \left(\sum_{j \in \{DG, grid\}} (E_j \cdot EF_j) \right) \quad (20)$$

where E_i denotes the annual energy production of component i , while η_i represents the efficiency factor for component

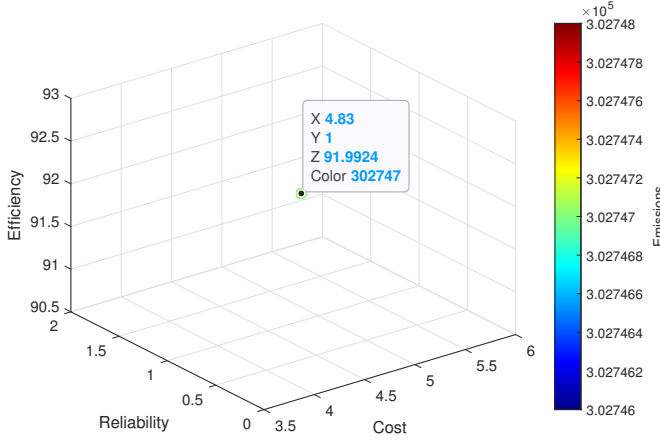


Fig. 4: Trade-off Among Cost, Reliability, Efficiency, and Emissions .

i. The term d_i signifies the annual degradation rate of the component i , and t indicates the year of operation. The emission factor of grid electricity, denoted by EF_{grid} , is quantified in kilograms of CO_2 per kilowatt-hour ($\text{kg CO}_2/\text{kWh}$). Similarly, E_j corresponds to the annual energy production or consumption of component j such as DGs or grid electricity, and EF_j represents the emission factor for component j in $\text{kg CO}_2/\text{kWh}$.

D. Input Parameters

The cost-effective design of MGs requires a comprehensive set of input parameters that accurately characterize the technical, economic, and operational aspects of the system. These parameters serve as the foundation for optimization algorithms and economic analyses, directly influencing the resulting MG configuration and performance.

- **Load Profiles:** Historical consumption data from the target community, sampled at hourly intervals over one year, capturing seasonal variations and peak demand periods. Also, the hourly load with variation of $\pm 20\%$ is considered throughout the year.
- **Resource Availability:** Monthly solar radiation profile and ordinary wind velocity of Central Tilba, NSW ($36^\circ 18.8'S, 150^\circ 04.6'E$) are considered for this work. Solar and wind resource data are obtained from the NASA prediction of Worldwide energy resource database. The monthly average solar radiation and wind speed for this region are shown in Fig. 3.
- **Grid Parameters:** The electricity purchase price from the utility grid under standard operating conditions, the sellback price for excess electricity exported to the grid, the maximum grid capacity for import/export operations, and peak pricing during high-demand periods are significant factors. These parameters substantially influence the economic operation of the MG and the optimal dispatch strategy, particularly in determining the utilization of stored energy versus grid imports.

- **Technical and Economic Parameters:** Table I presents the technical specifications and economic data for the principal MG components considered in this investigation. The data represent current market values based on manufacturer specifications and recent industry reports. In addition to the component costs delineated in Table I, this study considers the project financing terms and inflation rates over the project duration (25 years).

IV. RESULTS

This section provides a detailed evaluation the simulated MG configurations, revealing the multidimensional trade-offs among economic viability, system reliability, operational efficiency, and environmental impact in grid-connected community MG architectures.

A. Optimal Solutions

The multi-objective optimization framework presented in this study provides valuable insights into the trade-offs between cost, reliability, efficiency, and emissions in designing a cost-effective grid-tied community MG. The optimization results shown in Fig. 4 and Table II, demonstrate the impact of various design strategies on system performance and economic viability. The proposed design (A5) achieves a NPC of \$4.83M, 100% reliability, and 91.99% efficiency while maintaining a moderate emissions (ΔCO_2) level of 302,747 kg/year . This result indicates that the proposed MG configuration provides an optimal balance across all objectives. The system configuration comprises 418 kW of PV capacity, 123 kW of wind power, and 704 kWh of battery storage, eliminating reliance on a DG while attaining a LCOE of \$0.208/kWh.

B. Comparison with Conventional Designs

A comparative analysis with alternative designs provides significant insights into cost-effective MG designs. As depicted in Fig. 5, various design approaches prioritize distinct objectives, resulting in diverse system configurations and performance outcomes across cost, reliability, efficiency, and emissions. The findings are discussed in the subsequent subsections.

1) **Cost-Reliability Trade-off:** The cost-optimized design (A1) achieves the lowest NPC (\$4.47M) but compromises reliability ($\mathcal{R}_{sys} = 0.9994$). In contrast, the reliability-optimized design (A2) ensures complete reliability at a substantially higher cost (\$5.53M) due to the increased storage capacity (872 kWh). These findings demonstrate that attaining 100% reliability results in an exponential increase in costs, primarily attributed to the necessity for additional backup capacity.

2) **Efficiency vs. Cost Relationship:** The efficiency-optimized design (A3) achieves the highest efficiency (96.997%), but incurs a higher NPC (\$5.81M) and relies predominantly on wind generation (462 kW) and battery storage (640 kWh). This exemplifies the trade-off wherein maximizing efficiency requires increased investments in storage and renewable energy capacity, which may not always be economically viable.

TABLE II: Comparison of Different Design Approaches

Design Approach (A)	Selected Configuration					C_{np}	\mathcal{R}_{sys}	η_{sys}	ΔCO_2	Other Metrics		
	PV	WT	DG	BES	CON					LCOE	C_{OM}	C_{cap}
Cost-optimized (A1)	451kW	69kW	60kW	464kWh	293kW	4.47	0.9994	92.5	315909	0.19	189939	1.8M
Reliability-optimized (A2)	785kW	261kW	60kW	872kWh	324kW	5.53	1	79.744	31041	0.195	183291	2.24M
Efficiency-optimized (A3)	0	462kW	60kW	640kWh	206	5.81	0.9994	96.997	361807	0.252	243356	1.6M
Emission-optimized (A4)	1057kW	513kW	60kW	1176kW	549	6.06	0.9993	79.956	-382269	0.175	144142	3.57M
Proposed (A5)	418kW	123kW	0	704kW	255kW	4.83	1	91.9924	302747	0.208	201473	1.42M

3) *Emissions Reduction and Economic Viability:* The emission-optimized design (A4) achieved the lowest emissions (-382,269 kg), albeit at the highest NPC (\$6.06M) and the lowest efficiency (79.96%). This configuration relies on extensive renewable energy integration (1,057 kW PV and 513 kW wind), significantly reducing carbon emissions, but necessitating substantial capital investment (\$3.57M). In contrast, the proposed design (A5) achieves a 4.83% cost reduction while maintaining acceptable emissions and high efficiency, rendering it more feasible for practical applications.

4) *Proposed Design:* The proposed configuration (A5) demonstrated an optimal balance across all objectives, exhibiting 100% reliability, 91.99% efficiency, and moderate emissions of 302,747 kg/year. Compared to alternative approaches, it presents a well-balanced integration of renewable energy sources while maintaining economic viability and environmental benefits. The LCOE for the proposed design (\$0.208/kWh) is lower than that of the efficiency- and emission-optimized designs, ensuring economic feasibility. Furthermore, its Capital Expenditure of \$1.42M is lower than most other configurations, underscoring its cost-effectiveness in comparison to designs with high renewable energy penetration.

C. Sensitivity to Key Parameters

The performance of the proposed cost-effective MG design was evaluated under various system conditions to assess its reliability, efficiency, economic feasibility, and environmental impact. This section presents the key findings, including the system response to uncertainties in load demand and renewable energy generation, as well as the sensitivity of the LCOE to critical economic parameters. The results elucidate the trade-offs involved in optimizing cost, reliability, and sustainability, while ensuring the resilience of the MG against operational fluctuations.

1) *Sensitivity Analysis of System Performance Under Uncertainty:* The effects of uncertainty in the load demand, PV output, and wind output on the key system performance metrics are presented in Table III. These metrics include NPC (C_{NP}), reliability (\mathcal{R}_{sys}), efficiency (η_{sys}), and carbon emissions (ΔCO_2). The findings of this analysis demonstrate the resilience of the proposed MG design and its response to uncertainty.

- **Load Variations:** The system demonstrates a substantial cost and emission impact due to load fluctuations. A 10% increase in load results in a 5.87% increase in NPC and an 18.06% increase in emissions, as additional energy is required from storage or grid purchases. Conversely, a 10% reduction in load leads to an 8.66% reduction in NPC and a 26.2% decrease in emissions, illustrating

the direct correlation between demand and operational sustainability. The reliability remains constant ($\mathcal{R}_{sys}=1$), indicating that the system maintains full reliability under demand variations. However, efficiency marginally decreases under lower loads due to the underutilization of generation assets.

- **PV Output Variations:** A 10% increase in PV output results in a 3.05% reduction in NPC and an 11.3% reduction in emissions, demonstrating the economic and environmental advantages of increased solar generation. Conversely, a 10% reduction in PV output leads to a 3.05% increase in NPC and an 11.3% increase in emissions, indicating a greater dependence on backup generation. The efficiency improves with increased PV generation, while the reliability remains constant, further substantiating the robustness of the system.
- **Wind Output Variations:** The impact of wind fluctuations is less pronounced than that of PV variations, with a 10% increase in the NPC by 4.2% and emissions by 13.61%. A 10% decrease in wind output results in a modest 0.61% increase in NPC, suggesting that wind availability has a relatively moderate impact on the overall cost compared to PV fluctuations. The efficiency exhibits a slight decline with lower wind penetration, while the reliability remains consistent.

These findings indicate that, while the proposed MG demonstrates resilience to fluctuations in renewable energy generation, the optimization of PV penetration is more crucial than wind in ensuring cost-effectiveness and emission reduction. Demand-side management strategies can further mitigate the impact of load variations on the system sustainability.

2) *Sensitivity Analysis of LCOE:* the sensitivity of the LCOE to key economic parameters is illustrated in Fig. 6. The economic parameters considered in this test include electricity purchase price, sellback price, battery capital cost, and PV capital cost. The analysis reveals the relative influence of these parameters on the system economics.

- **Electricity Purchase Price:** The LCOE exhibits significant sensitivity to the electricity purchase price, with a 20% increase resulting in an approximately 10% increase in the LCOE. This observation suggests that grid electricity costs remain a predominant factor in the overall MG economics, underscoring the importance of self-sufficiency through optimized renewable energy integration.
- **Sellback Price:** The sellback price demonstrates a relatively minor influence on LCOE, indicating that revenue generated from excess energy exports does not substantially affect overall cost-effectiveness. This observation

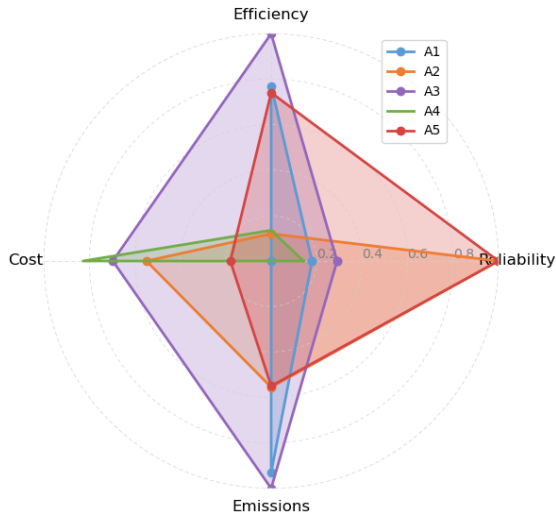


Fig. 5: Multi-objective Trade-offs for Different Optimization Priorities.

emphasizes the necessity for efficient on-site utilization and storage mechanisms rather than dependence on feed-in tariffs.

- **Battery and PV Capital Costs:** Battery capital costs demonstrate a more pronounced influence on LCOE compared to PV capital costs, as evidenced by the steeper slope in Fig. ???. A 20% increase in battery costs results in an approximately 5% increase in the LCOE, whereas PV cost variations yield a more gradual LCOE change. This observation suggests that battery storage optimization is critical for ensuring cost-effective MG operation, particularly in scenarios with high renewable energy penetration.

V. DISCUSSION

The results of this investigation demonstrate that an economically viable microgrid design can be achieved through a strategically balanced optimization approach, ensuring high reliability, efficiency, and emission control without disproportionate cost increases. The proposed approach provides a pragmatic and scalable design methodology for sustainable and economically viable MG operations, and serves as a benchmark for policymakers and energy planners. Although the optimization findings reveal significant technical and financial benefits, several practical aspects of the implementation require additional examination.

A. Exclusion of DGs and the Role of Large BESS

A crucial strategic decision in this study involves opting for a substantial BESS instead of DGs to guarantee complete reliability in the suggested microgrid setup. Although BESS provide substantial environmental and operational benefits by eliminating fossil fuel dependency, the findings indicate that high BESS capacity introduces trade-offs in terms of cost, flexibility, and long-term operational resilience during grid outages.

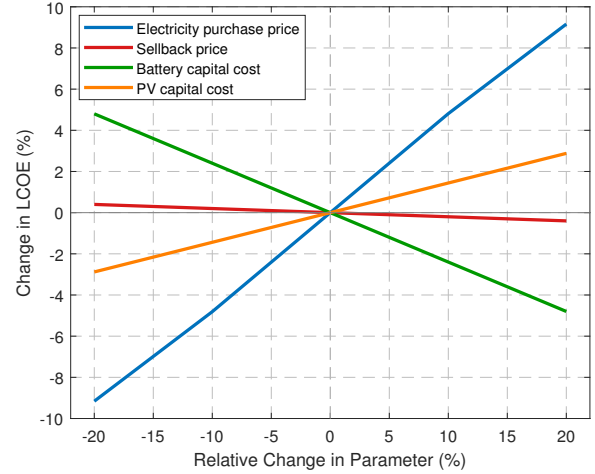


Fig. 6: Sensitivity Analysis of Key Parameters on LCOE.

1) *Operational Response Time:* DGs provide rapid response capabilities, particularly in high-load demand scenarios, where immediate power availability is critical. DGs can achieve full power output within seconds, rendering them suitable for managing sudden load surges and transient events. In contrast, battery storage systems rely on inverter-based power electronics, which may introduce minor delays in the response time, particularly under high-power ramping conditions.

2) *Long-Term Grid Outage Support:* During prolonged grid outages, the BESS is constrained by finite energy storage capacity. To maintain essential loads, the BESS requires adequate renewable energy generation and frequent recharge cycles. Although BESS can efficiently handle short-duration outages, however, their capacity limitations make them less viable for extended backup operations. Conversely, DGs can provide continuous power for prolonged periods, contingent on fuel availability, making them a more suitable option in regions with unreliable renewable resource availability.

Despite these advantages, in this study, the diesel-free approach is selected to mitigate emissions, reduce operational and maintenance costs, and enhance renewable energy penetration.

B. Economic Impact of Large BESS Capacity

Achieving 100% reliability without DG support requires a substantially larger BESS capacity (704 kWh in the proposed system). However, increased BESS sizing increases both the NPC and LCOE, as evidenced by the sensitivity analysis (Table II). The results indicate that an increase in BESS size directly correlates with higher capital expenditure, consequently increasing the LCOE and overall system cost, thus necessitating an optimal balance between storage sizing and economic viability. Furthermore, oversizing of the BESS may result in underutilized storage capacity during normal grid operation, thereby reducing the cost-effectiveness of the system.

TABLE III: Performance Variation of the Selected Optimal MG Design Under Different Uncertainties

Parameter	Uncertainty [%]	Metrics Deviation			
		C_{NP} [%]	\mathcal{R}_{sys} [%]	η_{sys} [%]	ΔCO_2 [%]
Load	-5	-5.15	0	-0.81	-15.19
	5	2.12	0	0.065	6.95
	-10	-8.66	0	-1.31	-26.2
	10	5.87	0	0.45	+18.06
PV Output	-5	-1.02	0	0.59	-0.05
	5	-2.44	0	-1.4	-7.93
	-10	0	0	1.56	4.5
	10	-3.05	0	2.44	-11.3
Wind Output	-5	-0.40	0	-0.31	0.34
	5	-3.05	0	-0.46	-8.81
	-10	0.61	0	-0.24	4.56
	10	-4.2	0	-0.53	-13.61

C. Implications for Future Microgrid Design

A potential hybrid approach integrating a small DG unit alongside a BESS could provide a cost-effective and reliable alternative, optimizing both short-term response and long-term backup capability while mitigating emissions. Future research should explore optimal DG-BESS hybrid configurations to achieve a balance between reliability, cost, and environmental performance. In addition, hydrogen-based backup solutions may offer long-duration energy storage with zero emissions as alternatives to conventional DGs.

VI. CONCLUSION

This study presents a cost-effective MG design that optimally balances the economic feasibility, reliability, efficiency, and environmental impact through a multi-objective optimization approach. Findings reported in this study shed new light on developing a comprehensive framework to supply secure, reliable, and affordable power in regional and remote areas. The results reveal that the proposed design achieves a C_{NP} of \$4.83M, ensuring high reliability ($\mathcal{R}=1$). The results also demonstrate that the η_{sys} of the proposed MG configuration is 91.99%, while maintaining carbon emissions at 302,747 kg/year. The economic evaluation further demonstrates that the proposed system attains a LCOE of \$0.208/kWh, with an annual operational expenditure of \$201,473 and capital investment of \$1.42M, rendering it more economically viable than alternative design approaches. The sensitivity analysis shows that load variations exert the most substantial influence on system emissions and cost, whereas PV output fluctuations impact economic and environmental performance to a greater extent than wind variations. Furthermore, the LCOE sensitivity analysis indicates that the electricity purchase price and battery capital costs constitute the most critical factors affecting the overall system cost, underscoring the necessity for efficient energy management strategies and optimized storage integration.

Therefore, incorporating energy management as a future extension of this study would be valuable, as it could further enhance MG resilience under real-time operational uncertainties.

ACKNOWLEDGMENT

The authors acknowledge University of New South Wales (UNSW), Australia for providing the financial supports to

perform this research.

REFERENCES

- [1] R. A. Mahuze, A. Amadeh, B. Yuan, and K. M. Zhang, "Collaborative optimization framework for capacity planning of a prosumer-based peer-to-peer electricity trading community," *Applied Energy*, vol. 384, p. 125289, 2025.
- [2] X.-Y. Zhang, C. Wang, J.-W. Xiao, and Y.-W. Wang, "A transactive energy cooperation scheduling for hydrogen-based community microgrid with refueling preferences of hydrogen vehicles," *Applied Energy*, vol. 377, p. 124582, 2025.
- [3] A. Bouaouda and Y. Sayouti, "An optimal sizing framework of a microgrid system with hydrogen storage considering component availability and system scalability by a novel approach based on quantum theory," *Journal of Energy Storage*, vol. 92, p. 111894, 2024.
- [4] S. S. Ottenburger, R. Cox, B. H. Chowdhury, D. Trybushnyi, E. A. Omar, S. A. Kaloti, U. Ufer, W.-R. Pogonietz, W. Liu, E. Deines *et al.*, "Sustainable urban transformations based on integrated microgrid designs," *Nature Sustainability*, vol. 7, no. 8, pp. 1067–1079, 2024.
- [5] M. M. Alam, M. Hossain, M. A. Zamee, and A. Al-Durra, "Design and operation of future low-voltage community microgrids: An ai-based approach with real case study," *Applied Energy*, vol. 377, p. 124523, 2025.
- [6] B. Liu, D. Wang, J. Huang, and C. Mao, "Optimal fnn-based energy management system with high real-time performance and good interpretability for battery in grid-connected microgrid," *IEEE Transactions on Industrial Electronics*, 2025.
- [7] N. N. Ibrahim, J. J. Jamian, and M. M. Rasid, "Optimal multi-objective sizing of renewable energy sources and battery energy storage systems for formation of a multi-microgrid system considering diverse load patterns," *Energy*, vol. 304, p. 131921, 2024.
- [8] J. Baum, P. Curtiss, J. Lee, M. Higginson, and B. Harwig, "Practical considerations for the design and control of networked microgrids: Enabling effective operation," *IEEE Electrification Magazine*, vol. 12, no. 2, pp. 22–32, 2024.
- [9] N. F. P. Dinata, M. A. M. Ramli, M. I. Jambak, M. A. B. Sidik, and M. M. Alqahtani, "Designing an optimal microgrid control system using deep reinforcement learning: A systematic review," *Engineering Science and Technology, an International Journal*, vol. 51, p. 101651, 2024.
- [10] F. C. Coelho, F. A. Assis, C. C. José Filho, A. R. Donadon, R. A. Roncolatto, V. E. Andrade, P. A. Rosas, S. L. Barcelos, O. R. Saavedra, R. G. Bento *et al.*, "Monte carlo simulation of community microgrid operation: Business prospects in the brazilian regulatory framework," *Utilities Policy*, vol. 92, p. 101856, 2025.
- [11] A. Valencia-Díaz, E. M. Toro, and R. A. Hincapié, "Optimal planning and management of the energy–water–carbon nexus in hybrid ac/dc microgrids for sustainable development of remote communities," *Applied Energy*, vol. 377, p. 124517, 2025.
- [12] L. He, S. Zhang, Y. Chen, L. Ren, and J. Li, "Techno-economic potential of a renewable energy-based microgrid system for a sustainable large-scale residential community in beijing, china," *Renewable and Sustainable Energy Reviews*, 2018.
- [13] J. Liu and Y. Bi, "System parameter design for community microgrid energy system based on a bi-level optimization model," *Volume 7: Energy*, 2023.
- [14] C. Yuan, M. Illindala, and A. Khalsa, "Co-optimization scheme for distributed energy resource planning in community microgrids," *IEEE Transactions on Sustainable Energy*, vol. 8, pp. 1351–1360, 2017.

- [15] S. Mohamed, M. Shaaban, M. Ismail, E. Serpedin, and K. Qaraqe, "An efficient planning algorithm for hybrid remote microgrids," *IEEE Transactions on Sustainable Energy*, vol. 10, pp. 257–267, 2019.
- [16] İ. Çetinbaş, B. Tamyürek, and M. Demirtaş, "Sizing optimization and design of an autonomous ac microgrid for commercial loads using harris hawks optimization algorithm," *Energy Conversion and Management*, vol. 245, p. 114562, 2021.
- [17] S. Jeyaprabha and J. Milanović, "Probabilistic techno-economic design of isolated microgrid," *IEEE Transactions on Power Systems*, vol. 38, pp. 5267–5277, 2023.
- [18] J. A. M. Alvarez, I. G. Zurbriggen, F. Paz, and M. Ordonez, "Microgrids multiobjective design optimization for critical loads," *IEEE Transactions on Smart Grid*, vol. 14, pp. 17–28, 2023.
- [19] X. Zhu, G. Ruan, H. Geng, H. Liu, M. Bai, and C. Peng, "Multi-objective sizing optimization method of microgrid considering cost and carbon emissions," *IEEE Transactions on Industry Applications*, vol. 60, pp. 5565–5576, 2024.
- [20] B.-C. Oh, Y.-G. Son, D. Zhao, C. Singh, and S.-Y. Kim, "A bi-level approach for networked microgrid planning considering multiple contingencies and resilience," *IEEE Transactions on Power Systems*, vol. 39, pp. 5620–5630, 2024.
- [21] G. Er, G. Soykan, and E. Canakoglu, "Stochastic optimal design of a rural microgrid with hybrid storage system including hydrogen and electric cars using vehicle-to-grid technology," *Journal of Energy Storage*, vol. 75, p. 109747, 2024.
- [22] C. Yan, Y. Zou, Z. Wu, and A. Maleki, "Effect of various design configurations and operating conditions for optimization of a wind/solar/hydrogen/fuel cell hybrid microgrid system by a bio-inspired algorithm," *International Journal of Hydrogen Energy*, vol. 60, pp. 378–391, 2024.
- [23] P. Odonkor and S. Ashmore, "Regional performance analysis of residential microgrids: A multi-factor assessment of cost, resilience, and environmental impact," *Energy and Buildings*, p. 115433, 2025.
- [24] M. Eklund, A. Voinov, M. Hossain, and K. Khalilpour, "Evaluating the interplay of community behaviour and microgrid design through optimisation modelling in local energy markets," *Renewable and Sustainable Energy Reviews*, vol. 210, p. 115271, 2025.
- [25] M. Uddin, H. Mo, D. Dong, S. Elsawah, J. Zhu, and J. M. Guerrero, "Microgrids: A review, outstanding issues and future trends," *Energy Strategy Reviews*, vol. 49, p. 101127, 2023.
- [26] G. Shafiullah, M. Amanullah, A. S. Ali, D. Jarvis, and P. Wolfs, "Prospects of renewable energy—a feasibility study in the Australian context," *Renewable Energy*, vol. 39, no. 1, pp. 183–197, 2012.
- [27] P. A. Cordero, J. L. García, and F. Jurado, "Optimization of an off-grid hybrid system using lithium ion batteries," *Acta Polytechnica Hungarica*, vol. 17, no. 3, pp. 185–206, 2020.